

Brief Communication: Thinning of debris-covered and debris-free glaciers in a warming climate

Argha Banerjee

Earth and Climate Science, Indian Institute of Science Education and Research Pune, Pune 411008, India

Correspondence to: Argha Banerjee (argha@iiserpune.ac.in)

1 **Abstract.** Recent geodetic mass balance measurements reveal similar thinning rates in glaciers with or without debris cover
2 in the Himalaya-Karakoram region. This comes as a surprise as a thick debris cover reduces the surface melting signifi-
3 cantly due to its insulating effects. Here we present arguments, supported by results from numerical flowline model sim-
4 ulations of idealised glaciers, that a competition between the changes in the surface mass balance forcing and that of the
5 emergence/submergence velocities can lead to similar thinning rates with or without the debris. The thinning rate on a debris-
6 covered glacier is initially smaller than that of a similar debris-free glacier. Subsequently the thinning rate in the debris-covered
7 glaciers becomes comparable to and then larger than that in the debris-free glacier. The time evolution of the glacier averaged
8 thinning rates after an initial warming is strongly controlled by time-variation of the emergence velocity profile.

9 1 Introduction

10 A knowledge-gap related to debris-covered glacier dynamics affects our understanding of the past and future of Himalayan
11 glaciers in a changing climate (Scherler et al , 2011). A supra-glacial debris cover present over the ablation zone of any glacier
12 induces qualitative changes in its response (Naito et al , 2000; Vacco et al , 2010; Banerjee and Shankar , 2013; Anderson and
13 Anderson , 2015) due to a suppressed melt-rate under a thick debris layer (Nakawo and Young , 1982; Mattson et al , 1993).
14 Where as a thin debris cover is expected to accelerate melt, due to its low albedo. While responding to a warming climate,
15 debris-covered glaciers exhibit a larger climate sensitivity, longer response time (Banerjee and Shankar , 2013), a decoupling
16 of volume and length change, and formation of a slow-flowing stagnant downwasting tongue (Scherler et al , 2011; Banerjee
17 and Shankar , 2013). Despite several efforts to model and understand the dynamics of debris-covered glaciers with various
18 degrees of sophistication (Naito et al , 2000; Vacco et al , 2010; Banerjee and Shankar , 2013; Anderson and Anderson , 2015;
19 Rowan et al , 2015), challenges still remain. This task is made more difficult by our limited understanding of the time-evolution
20 of the debris extent (Anderson and Anderson , 2015), the variability of debris thickness, and common occurrences of highly
21 dynamic supraglacial ponds and ice-cliffs that cause intense localised melting (Sakai et al , 2000; Miles et al , 2015; Steiner et
22 al , 2015).

23 A curious fact that has emerged in the large scale remote sensing measurements of glaciers in the Himalaya and Karakoram
24 during the first decade of 21st century (Kääb et al , 2012; Gardelle et al , 2012; Nuimura et al , 2012; Gardelle et al , 2013) is
25 the similar magnitude of thinning of glacial ice irrespective of the presence of supraglacial debris-cover. This seems counter-

1 intuitive. A thick debris cover, due to its insulating properties, significantly inhibits the melt of underlying ice - so much so
2 that in the debris-covered part of the glacier, specific melt-rate does not increase with decreasing elevation. Rather, it reaches a
3 saturation value or even decreases (Banerjee and Azam , 2015) on the lower reaches of the glacier. Why then should both the
4 glacier-types experience similar rate of thinning as climate warms up?

5 Heuristic arguments were offered by various authors to reconcile with this apparent paradox. Kääb et al (2012) suggested
6 that the insulating effect of the debris cover might be compensated for at the scale of the whole ablation zone, due to enhanced
7 melting at the thermoskarst features, namely, supra-glacial ponds and ice-cliffs that are often present in debris covered glaciers.
8 These features, due to the discontinuous debris cover, experience large localised melting. Given that these features typically
9 contribute $\sim 10 - 20\%$ of the total melt (Sakai et al, (2000); Reid and Brock, (2014)) , it is unlikely that they can lower the
10 glacier wide mean melt rate in the debris-covered glaciers sufficiently so as to match that of the debris-free glaciers. Field
11 measurements by Vincent et al (2016) seems to confirm this. It was also conjectured that a reduction of ice flux from upstream
12 areas to a stagnant tongue may be behind this larger-than-expected thinning of debris-covered glacial ice (Kääb et al , 2012;
13 Gardelle et al , 2012). Nuimura et al (2012) too mentioned the possible role of reduced flux at low-slope slow-moving stagnant
14 tongue of large debris-covered glaciers, but a quantification of this flux-effect is missing as yet.

15 On the other hand, Banerjee and Shankar (2013) showed that a reduced melt-rate in the debris-covered tongue does not
16 affect the nature of volume response of the glacier qualitatively, in stark contrast with its drastic effect on the length response.
17 However, their model results (figure 3d of Banerjee and Shankar (2013)) show larger thinning rate in debris-free glaciers.
18 Further, it was reported that in the Pamir-Karakoram-Himalaya, depending on the region chosen, geodetic measurement gives
19 decadal thinning rate of ice under a debris cover that are either larger or smaller than, or similar to that of debris-free ice
20 (Gardelle et al , 2013). The present scenario is summed up neatly by Vincent et al (2016), “This question of area-averaged
21 melting rates over debris-covered or clean glacier ablation areas remains unanswered”.

22 In this contribution, we analyse the rate of thinning in debris-covered and debris-free glaciers in a warming climate, using
23 a simplified one-dimensional flowline model of idealised glaciers (Banerjee and Shankar , 2013; Banerjee and Azam , 2015).
24 We conduct a few simple numerical experiments to investigate the role of the magnitude of warming rate, ice dynamics (i.e.
25 the changes in flux gradients or equivalently the changes in emergence/submergence velocities) and that of the surface mass
26 balance, in controlling the thinning rates in these two glacier types.

27 **2 Glacier response to instantaneous warming**

28 An easy-to-analyse piece of this problem is the behaviour of a steady-state debris-covered or debris-free glacier immediately
29 after an instantaneous rise of temperature (or equivalently of equilibrium line altitude (ELA)). In a steady state, the ice-
30 thickness profile is kept steady due to a stable balance between the surface ablation (accumulation) rate and the emergence
31 (submergence) velocities. Dictated by mass conservation of incompressible ice, the emergence or submergence rate equals the
32 negative gradient of the flux, $F(x)$. After an instantaneous change in ELA, the surface mass balance values change, but ice
33 flow takes a characteristic longer time to relax. Therefore, the initial local thinning rate is just the difference in specific mass

1 balance, $B(x)$, before and after the change in temperature. However this is valid only over a time scale short compared to the
2 above flow-relaxation time.

3 Let us consider two idealised model glaciers. Glacier A is without debris and has a linear mass-balance profile. Glacier
4 B has supraglacial debris cover and the ablation rate saturates to a value of -2 m/yr in the debris-covered region (figure 1b).
5 This idealised mass-balance profile for the debris covered glacier is motivated by data from Himalayan glaciers (Banerjee
6 and Azam , 2015). Similar simplified mass-balance profiles have been used to analyse the response of the debris-covered
7 Himalayan glaciers (Banerjee and Shankar , 2013; Banerjee and Azam , 2015). In a real glaciers, possible variability of the
8 debris thickness and ephemeral thermokarst features (ponds and ice-cliffs) cause significant spatial variation of the melt-rate in
9 the debris covered parts of the glacier. However, a relatively fast advection of these surface features would imply that a long-
10 term mean melt-rate at a specific location is a well defined quantity. This justifies the simplified mas-balance profile employed
11 here. Further, the observed thinning rate values in the Himalaya are obtained for a large set of glaciers. So possible effects of
12 specific details of mass-balance profile of individual glaciers would be averaged out.

13 In figure 1a, 1b we show mass-balance profile for the idealised model glaciers before and after an instantaneous rise of ELA,
14 $\Delta E = 50$ m. It is assumed here that the mass-balance shape remains the same and only change is through that of ELA (Banerjee
15 and Shankar , 2013). In practice, the debris layer may thicken and debris-covered area may grow in a warming climate, affecting
16 the shape of the melt-rate profile. However, it is known that above a debris thickness of ~ 10 cm, the decrease in melt-rate with
17 a thickening debris layer is small (Juene et al , 2014). Therefore such changes can safely be neglected as a first approximation.
18 The possible changes in supraglacial ponds/ice-cliffs are not important due to a relatively smaller contribution of these features
19 to the total melt, as argued in before. This assumption of an invariant shape allows for possible increase in debris extent with
20 warming as the upper boundary of the region with saturated melt-rate moves up with the ELA.

21 As is clear from the figure 1a, glacier A responds with a uniform glacier-wide thinning rate, $\langle \frac{dh}{dt} \rangle_A = \beta \Delta E$, right after the
22 change. Here β is the mass-balance gradient. For glacier B, a uniform thinning operates only in the debris-free upper part of
23 the glacier and the lower part has not thinned at all (figure 1b). Thus, glacier B has a lower mean thinning rate to start with,
24 $\langle \frac{dh}{dt} \rangle_B = (1 - f_d) \beta \Delta E$, where f_d is the debris-covered fraction. Remarkably these expressions should work independent of
25 the length of the glaciers. Also, the initial lack of thinning in the debris-covered glacier is independent of the actual value of
26 the melt-rate (assumed to be 2 m/yr here) under the thick debris layer and depends only on the general shape of the melt-curve
27 (figure 1b).

28 A more general mass-balance profile for a debris-covered glacier than the one considered above, would involve a smaller or
29 inverted mass-balance gradient in the debris-covered parts (Banerjee and Azam , 2015). Even then, the mean thinning rate of
30 this glacier would be less compared to its debris-free counterpart. In case of an inverted mass-balance, a transient thickening
31 of the lower ablation zone is obtained, though this is likely to be an artifact of the assumed fixed shape of mass-balance curve.
32 Above delayed thinning of the debris-covered terminus is consistent with the formation of a slow-flowing stagnant tongue with
33 a steady length commonly seen in the debris-covered glaciers in the Himalaya-Karakoram (Scherler et al , 2011), which raises
34 confidence in our minimal description of these glaciers.

35 Thus, a debris-covered glacier starts with a lower value of mean thinning rate compared to a debris-free one (as $\langle \frac{dh}{dt} \rangle_A >$
1 $\langle \frac{dh}{dt} \rangle_B$). The ice fluxes then respond to the mass-balance change and the subsequent evolution of flux gradient (or equivalently
2 the emergence velocity) profile alters the thinning rate distribution. Though the detailed pattern of the subsequent changes in
3 thinning rate is difficult to predict, at some later stage the thinning rate would decrease in glacier A and may become smaller
4 than that in glacier B which has to shed more mass due to a larger climate sensitivity (Banerjee and Shankar, 2013). If that is
5 the case, then there must be an intermediate crossover period during which the thinning rates in both the glaciers are similar
6 within measurement errors. This hypotheses is to be tested against numerical simulation of synthetic glaciers.

7 3 Numerical investigations

8 To verify above claims on the evolution of mean thinning rates in glacier A and B, we perform a set of numerical experiments
9 with 1-d flowline models of glacier A and B. The model glaciers have bedrock slope of 0.1, mass balance gradient $\beta = 0.007$
10 yr^{-1} . See Banerjee and Shankar (2013) for further details of the flowline model used. Note that these glaciers are identical
11 above the debris-covered region. The initial steady-states are prepared by running the models with an initial fixed value of
12 ELA for 500 (900) years for glacier A (B). The steady length of glaciers studied are in the range 6–14 km. Subsequently, the
13 following ELA perturbations are switched on at $t = 0$:

- 14 1. An instantaneous rise by 50 m.
- 15 2. A total rise of 50 m in steps of 5 m every five year.
- 16 3. A total rise of 30 m in steps of 1 m every five year.

17 In all the three experiments the net warming is similar, but the rates are different (infinite, 10 m/decade, and 2 m/decade
18 respectively). In experiment (3), we limit the total ELA rise to 30 m so as to limit the duration of the experiment to 150 years
19 for the sake of easy comparison with the other two experiments.

20 3.1 Results and discussions

21 3.1.1 Initial thinning rates

22 Just as argued in section 2, the mean thinning rate profiles obtained after a year in experiment (1) show uniform thinning
23 rate all over glacier A and in the upper part of glacier B (figure 1c, 1d). In contrast the debris-covered parts of glacier B
24 shows zero thinning. At this point, the flux gradient profile (same as the negative of emergence velocity), $\frac{dF}{dx}$, has not changed
25 significantly from the initial steady mass balance profile $B(x)$ (figure 1e, 1f). Further, the initial thinning rate for glaciers A
26 and B in experiment (1) are quite accurately given by $\beta\Delta E$ (0.35 m/yr) and $(1 - f_d)\beta\Delta E$ (0.22 m/yr) respectively. All these
27 results are consistent with our arguments outlined in section 2. The thinning rate trends for finite warming rates follow similar
28 pattern, with the difference between two thinning rates during the initial phase growing with the warming rate value (figure 2;
29 experiments (2) and (3)).

1 3.1.2 Time evolution of thinning rates

2 The thinning of ice results from a difference between local melt-rate and the corresponding emergence velocity. Data from
3 experiment (1) shows that the initial profile of thinning rate gets modified at later times largely due to the changes in the profile
4 of $\frac{dF}{dx}$ (figure 1e, 1f). After the initial applied change, the competing term of mass balance rate varies weakly with time - only
5 due to a feedback from changing thickness. Therefore, the evolution of the spatial distribution and the mean value of thinning
6 rate is mostly dynamically controlled, due to a changing emergence velocity profile. This is true for both the glaciers types.

7 Consistent with arguments given in section 2, initial low values of glacier-averaged thinning rate in glacier B, matches and
8 then overtakes that of glacier B (figure 2) with time. That is, depending on the stage of response, a debris-covered glacier can
9 show smaller, larger or similar mean thinning rate as compared to that of a similar debris-free glacier. As expected, similar
10 trends are obtained in experiments with finite warming rates as well. However, at the limit of a very low rate of warming, the
11 thinning rate differences are small (figure 2; experiment(3)). The cross-over time seem to be controlled by the rate of warming.

12 While we have considered the glacier wide thinning rate, the same conclusions are obtained if one compares the lower part
13 of the two glaciers as they are identical in their upper parts. The thinning rates measured on a regional scale is an average over
14 glaciers with differences in size, bedrock-profile, and history of warming as well. Clearly, this may lead to larger, smaller or
15 similar mean thinning rates in the two glacier types from the same region, in agreement with observations by Gardelle et al
16 (2013).

17 4 Conclusions

18 We provide very general arguments that debris-covered glaciers can have smaller, larger or similar thinning rates responding
19 to a warming climate as compared to debris-free glaciers. The thinning rate is controlled by a competition between changing
20 mass-balance and emergence velocity profiles. A debris-covered glacier starts with a smaller glacier averaged thinning rate,
21 but overtakes that of debris-free glacier at later stages. The initial difference in the corresponding warming rates depend on the
22 balance gradient and debris-covered fraction. Our arguments are validated against results from flowline model simulations of
23 idealised glaciers. The numerical analysis show that the change in local melt-rates controls the thinning immediately after an
24 instantaneous warming, whereas a stronger variation of the corresponding emergence velocity profile dictates the evolution of
25 the thinning rate at subsequent stages.

26 *Acknowledgements.* This work is supported by DST-SERB grant no SB.DGH-71.2013.

1 References

- 2 Anderson, L. S., and R. S. Anderson. "Modeling debris-covered glaciers: extension due to steady debris input." *Cryosphere Discussions* 9.6
3 (2015).
- 4 Banerjee, A., and Azam, M. F. (2015). Temperature reconstruction from glacier length fluctuations in the Himalaya. *Annals of Glaciology*.
5 57 (71)
- 6 Banerjee, A., and Shankar, R. (2013). On the response of Himalayan glaciers to climate change. *Journal of Glaciology*, 59(215), 480-490.
- 7 Gardelle, J., Berthier, E., and Arnaud, Y. (2012). Slight mass gain of Karakoram glaciers in the early twenty-first century. *Nature geoscience*,
8 5(5), 322-325.
- 9 Gardelle, J., Berthier, E., Arnaud, Y., and Kaab, A. (2013). Region-wide glacier mass balances over the Pamir-Karakoram-Himalaya during
10 1999-2011 (vol 7, pg 1263, 2013). *Cryosphere*, 7(6).
- 11 Juen, M., Mayer, C., Lambrecht, A., Han, H., and Liu, S. (2014). Impact of varying debris cover thickness on ablation: a case study for
12 Koxkar Glacier in the Tien Shan. *The Cryosphere*, 8(2), 377-386.
- 13 Kääb, A., Berthier, E., Nuth, C., Gardelle, J., and Arnaud, Y. (2012). Contrasting patterns of early twenty-first-century glacier mass change
14 in the Himalayas. *Nature*, 488(7412), 495-498.
- 15 Mattson LE, Gardner JS and Young GJ (1993) Ablation on debris covered glaciers: an example from the Rakhiot Glacier, Punjab, Himalaya.
16 IAHS Publ. 218 (Symposium at Kathmandu 1992 - Snow and Glacier Hydrology), 289-296
- 17 Miles, E. S., Pellicciotti, F., Willis, I. C., Steiner, J. F., Buri, P., and Arnold, N. S. (2016). Refined energy-balance modelling of a supraglacial
18 pond, Langtang Khola, Nepal. *Annals of Glaciology*, 57(71), 29.
- 19 Naito N, Nakawo M, Kadota T and Raymond CF (2000) Numerical simulation of recent shrinkage of Khumbu Glacier, Nepal Himalayas.
20 IAHS Publ. 264 (Symposium at Seattle 2000 - Debris-Covered Glaciers), 245-254
- 21 Nakawo M and Young G J (1982). Estimation of glacier ablation under a debris layer from surface temperature and meteorological variables.
22 *Journal of Glaciology*, 28 (92), 29–34.
- 23 Nuimura, T., Fujita, K., Yamaguchi, S., and Sharma, R. R. (2012). Elevation changes of glaciers revealed by multitemporal digital elevation
24 models calibrated by GPS survey in the Khumbu region, Nepal Himalaya, 1992–2008. *Journal of Glaciology*, 58(210), 648-656.
- 25 Reid, T. D., and Brock, B. W. (2014). Assessing ice-cliff backwasting and its contribution to total ablation of debris-covered Miage glacier,
26 Mont Blanc massif, Italy. *Journal of Glaciology*, 60(219), 3-13.
- 27 Rowan, A. V., Egholm, D. L., Quincey, D. J., and Glasser, N. F. (2015). Modelling the feedbacks between mass balance, ice flow and debris
28 transport to predict the response to climate change of debris-covered glaciers in the Himalaya. *Earth and Planetary Science Letters*, 430,
29 427-438.
- 30 Sakai, A., Takeuchi, N., Fujita, K., and Nakawo, M. (2000). Role of supraglacial ponds in the ablation process of a debris-covered glacier in
31 the Nepal Himalayas. *IAHS PUBLICATION*, 119-132.
- 32 Scherler D, Bookhagen B and Strecker MR (2011) Spatially variable response of Himalayan glaciers to climate change affected by debris
33 cover. *Nature Geosci.*, 4(3), 156-159 (doi: 10.1038/ngeo1068)
- 34 Steiner, J. F., Pellicciotti, F., Buri, P., Miles, E. S., Immerzeel, W. W., and Reid, T. D. (2015). Modelling ice-cliff backwasting on a debris-
35 covered glacier in the Nepalese Himalaya. *Journal of Glaciology*, 61(229), 889-907.
- 36 Vacco, D. A., Alley, R. B., and Pollard, D. (2010). Glacial advance and stagnation caused by rock avalanches. *Earth and Planetary Science*
37 *Letters*, 294(1), 123-130.

1 Vincent, C., Wagnon, P., Shea, J. M., Immerzel, W. W., Kraaijenbrink, P. D. A., Shrestha, D., Soruco, A., Arnaud, Y., Brun, F., Berthier, E.,
2 and Sherpa, S. F.: Reduced melt on debris-covered glaciers: investigations from Changri Nup Glacier, Nepal, *The Cryosphere Discuss.*,
3 doi:10.5194/tc-2016-75, in review, 2016.

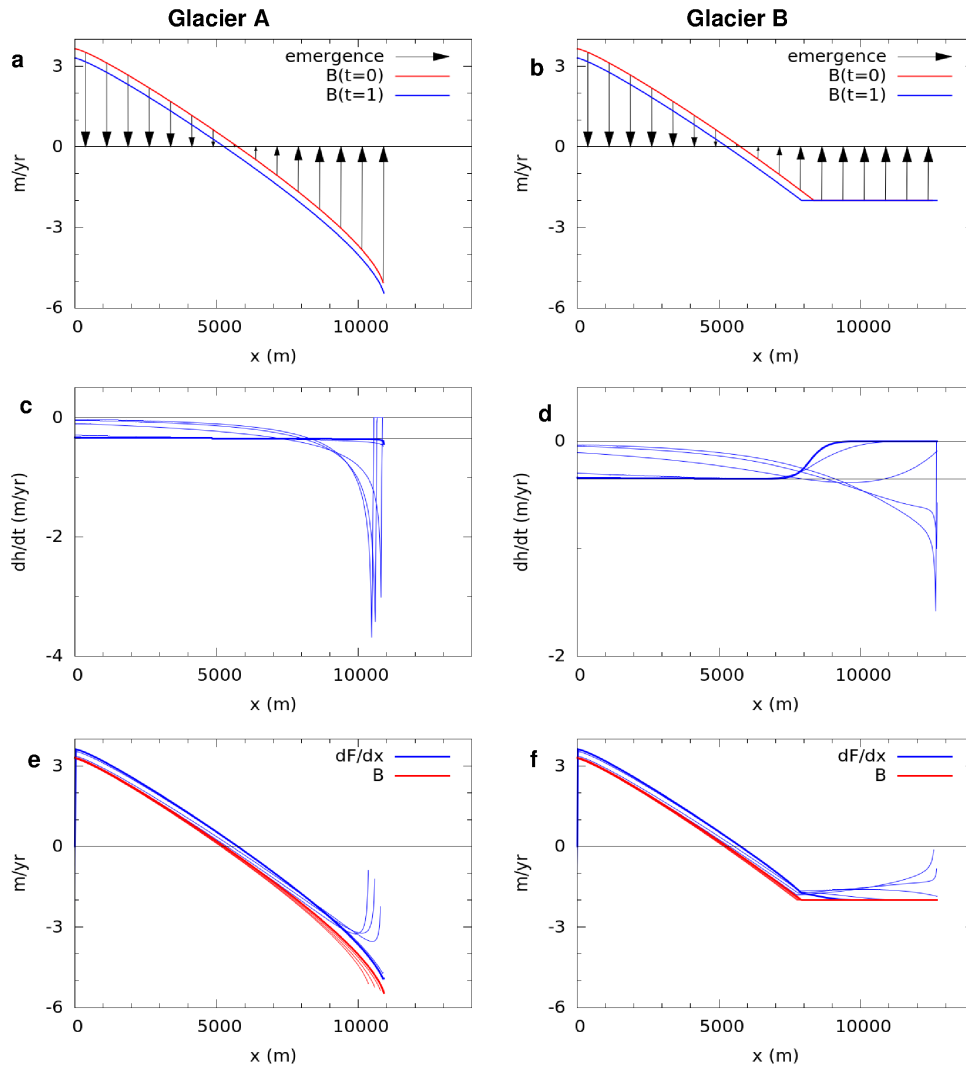


Figure 1. (a,b) The specific mass-balance as a function of position for the initial steady-states of the glacier A and B (red lines), with black arrows showing emergence velocities that balances surface mass balance at $t = 0$ year. The blue lines are the surface mass-balance profiles a year after a step change in ELA by 50m. (c,d) The thinning rate profiles after 1 (thick line), 5, 25, 45, and 65 years (thin lines). Note the different vertical scales and horizontal black thin lines at $\beta\Delta E = 0.35$ m/yr (see text for details). (e,f) Specific mass-balance (red) and flux gradient (blue) profiles after 1 (thick line), 5, 25, 45, and 65 years (thin lines).

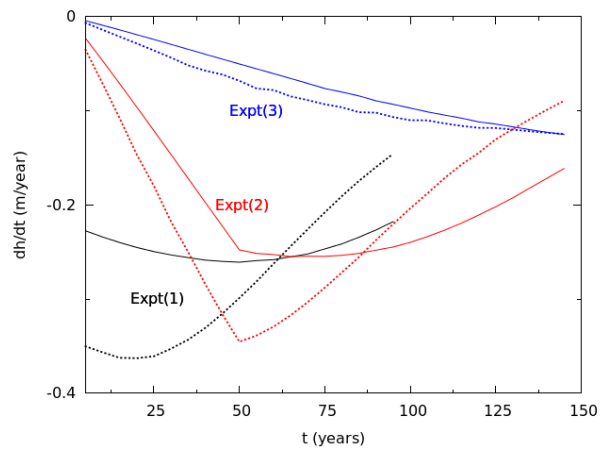


Figure 2. Evolution of thinning rate after ELA perturbations are applied to a model debris-covered glacier (solid line) and a debris-free glacier (dotted line). The warming rate profile for each of the experiment is described in section 3.